Rev.Adv.Mater.Sci. 11 (2006) 1-18

CHEMICAL PREPARATION OF SPECIAL-SHAPED METAL NANOMATERIALS THROUGH ENCAPSULATION OR INDUCEMENT IN SOFT SOLUTION

Chang Chen, Li Wang, Guohua Jiang and Haojie Yu

State Key Laboratory of Polymer Reaction Engineering, College of Materials Science and Chemical Engineering, Zhejiang University, Hangzhou 310027, People's Republic of China

Received: May 12, 2005

Abstract. It is reviewed the recent progress on the preparation of special-shaped metal nanomaterials including wires, rods, cubes, prisms, disks, and dendrites via chemical reduction in the presence of polymers or surfactants under the mild conditions. These polymers and surfactants act as capping agents or induce agents to control the anisotropic growth of metal crystals. It is found that many metal nanomaterials including silver, gold, copper, and other kinds of metal like platinum, lead, iron can be prepared via this approach. The growth mechanisms of special-shaped crystal are discussed detailedly. The application of resultant special-shaped metal nanomaterials is introduced briefly. Finally, we supply some personal perspectives on the future development of chemical preparation of special-shaped metal nanomaterials in soft solution.

1. INTRODUCTION

The materials with nanometer sizes in one, two or three dimensions have the unique physical, chemical and mechanical properties that are neither those of bulk materials nor those of molecular compounds [1]. And they have been exploited for the extensive potential applications in optics [2-4], electronics [4-5], magnetics [6], catalysts [7], chemical sensing [8], biomedicine [9-12], microreactor [13-14] and etc. These peculiar and fascinating properties of nanomaterials strongly depend on the particle size, the interparticle distance and the shape of the nanoparticles, so that controllable preparation of nanomaterials is very important and significative. Especially special-shaped nanomatel developed quickly recently and has become the focus of intensive research owing to its unique application of nanoscale devices and materials superior to their sphere shaped counterparts [15]. To obtain special-shaped nanomaterials, many physical and chemical approaches have been developed. Generally speaking, the physical approach produces nanomaterials from bulk materials with the help of exact and sophisticated equipments, while the chemical approach prepares nanomaterials from atoms or molecules through simpler and economical chemical routes. Therefore in the past decade, many research groups dedicated themselves to the chemical preparation of metal nanomaterials [16-21]. Usually, chemical approaches can be classified as four kinds: selfstructure confinement approach, hard or soft template approach, physical chemistry approach and soft solution approach. The selfstructure confinement approach is a facility route but only fits a limit set of solid materials. The template approach is a good control over the uniformity

Corresponding author: Li Wang, e-mail: opl_wl@dial.zju.edu.cn

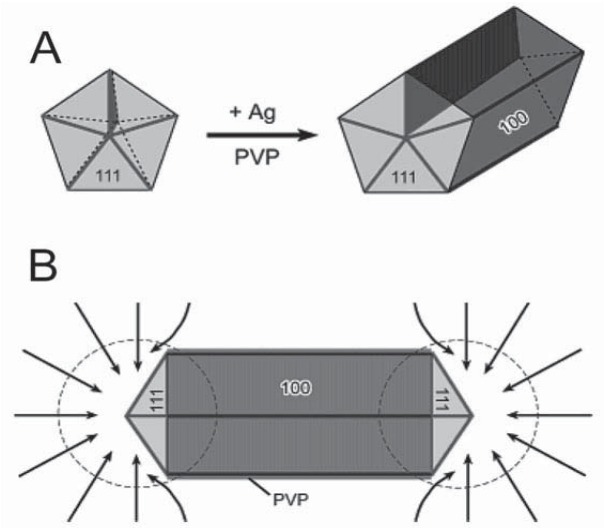

Fig. 1. Schematic illustration of the mechanism proposed to account for the growth of silver nanowires with pentagonal cross sections: (A) Evolution of a nanorod from a multiply twinned nanoparticle (MTP) of silver under the confinement of five twin planes and with the assistance of PVP. (B) Diffusion of silver atoms (arrows) toward the two ends of a nanorod, with the side surfaces completely passivated by PVP. Reproduced with permission from [22], copyright 2003, American Chemical Society.

and dimension route but it needs prefabricated templates, furthermore the removal of hard template is also difficult. The physical chemistry approach including electrochemistry, photochemistry, sonochemistry, radiolysis, thermolysis and *etc.* is considered as effective route, but requires more special equipments and higher cost. The soft solution approach can be defined as producing nanomaterials through chemical reduction under mild conditions in the presence of chemical additives like line-polymers [22-23], surfactants [24-32], dendrimers [33-41], these additives adsorb with metal irons firstly and then act as anisotropic confinements to induce and maintain anisotropic crystal growth by selective passivation of certain facets. This approach is able to generate special-shaped nanostructures with highly crystalline and well-controlled composition in a high yield, and it is considered as the preponderant route to put into large-scale industrial production because of its simple technology, mild production conditions and the lower cost.

This article reviews recent research progress on chemical preparation of special-shaped metal nanomaterials including silver, gold, copper, platinum, lead, and iron with the help of surface capping or induce agents in soft solution to obtain nanostructures such as wires, rods, cubes, prisms, disks, dendrites and *etc.*

2. CHEMICAL PREPARATION OF SPECIAL-SHAPED METAL NANOMATERIALS

2.1. Chemical preparation of special-shaped sliver nanomaterials

Silver has the highest electrical conductivity in the bulk metal, and its unusual properties depend on nanoparticle size, shape, composition, crystallinity, uniformity and structure (solid versus hollow). Many research groups try to achieve precise control over these properties of the metal nanomaterials. Xia *et al.* [42] demonstrated a polyol method to generate silver nanostructures especially nanowires by reducing silver nitrate with ethylene glycol (EG) in the presence of poly(vinylpyrrolidone) (PVP). The application of PVP as a polymeric capping reagent to kinetically control the growth rates of various faces of silver crystal is the key of the formation of the anisotropic nanostructures within a highly isotropic medium, it is found that the introduction of a seeding step to serve as nuclei for the subsequent growth of silver is very important to generate silver nanowire. A plausible growth mechanism has been developed for the polyol synthesis of uniform silver nanowire [22]. Murphy *et al.* [31] and Gai *et al*. [32] have proposed a mechanism in which gold nanorods were assumed to evolve from multiply twinned particles (MTPs) with a decahedral shape. Herein the con-

cept of MTP can also be introduced in the study of silver nanowires. The MTP has 5-fold symmetry, with its surface bounded by ten {111} facets. In terms of surface-energy minimization, it is favorable to form such a twinned nanostructure once the particle size has reached a critical value. A set of five twin boundaries are required to generate the decahedral particle because it is impossible to fill the space of an object of 5-fold symmetry with only a single-crystalline lattice [43]. Fig. 1 shows a schematic illustration of the mechanism for the growth of silver nanowire at the initial stage of the Ostward ripening. The ends of this nanorod are terminated by {111} facets, and the side surfaces are bounded by {100} facets. The strong chemical interaction between the oxygen (and/or nitrogen) atoms of the pyrrolidone units of PVP and the {100} facets of silver crystal is indicated with a dark-gray color, and the weak interaction with the {111} facets is ked by a light-blue color, these different interactions make the crystal seeds grow into nanmarorods or nanowires. The red lines on the end surfaces represent the twin boundaries with highest-energy can serve as active sites for the addition of silver atoms. The plane marked in red shows one of the five twin planes do not twist or bend during the entire growth process that can serve as the internal confinement for the evolution of nanorods from MTPs. Once the rod-shaped structure has been formed, it can readily grow into a longer nanowire because its side surfaces are tightly passivated by PVP and its ends are largely uncovered and remain to be attractive toward new silver atoms [22].

Recently, Xie *et al.* [44] ameliorate the mechanism above-mentioned and provided several evidences. They found out that the molecule ratio of PVP and silver atoms on the outer surface of nanowires is about 1.38 through analysis of TGA test and logical deduction bases on the pentagonal model (as shown in Fig. 2), so it can be demonstrated that there is only one monolayer of PVP adsorbed on the surfaces of silver nanowires. The results from Fourier transform Raman spectra (FT-Raman) can also confirm that the oxygen atom of PVP coordinates with silver atom on the surface through the nonbonding electrons, and it is suggested that the skeleton chain (CH_2 chain) of PVP is close to the surface of nanowires, simultaneously the pyrrolidone ring may be tilted on the same surfaces.

Several literatures reported that the protective mechanism of PVP in the electrochemical synthesis of silver particles is generally proposed on the basis of its structural features. PVP has a structure

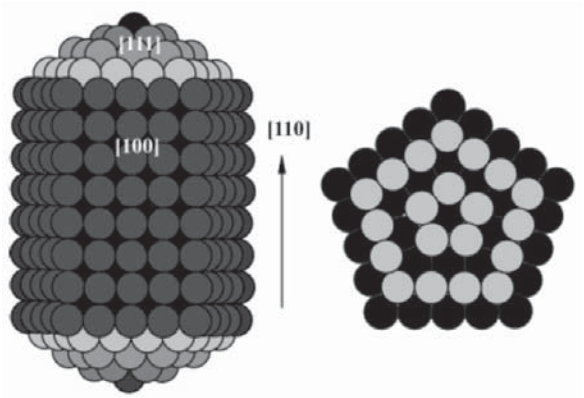

Fig. 2. Schematic pentagonal model of silver MTP, the amounts of silver atoms outer can be calculate by the value of nanowire diameter and this model. Reprinted with permission from [44], copyright 2004, American Chemical Society.

of a polyvinyl skeleton with polar groups [45]. The donated lone pairs of both nitrogen and oxygen atoms in the polar groups of one PVP unit may occupy two sp orbitals of silver ions to form a complex compound: the Ag_m^{m+}-PVP complex, in which *m* is the number of silver ions anchored at a PVP molecule. This case occurs in the chemical reduction process of silver ions in the presence of PVP [45-47]. Since the nitrogen and oxygen atoms of pyrrolidone in PVP contributes more electronic density to the sp orbital of silver ions than the oxygen atom of water does, the silver ions in the Ag_m^{m+}-PVP complex may obtain electrons more easily from the system than those in the Ag^+-H_2O complex. Thus, the presence of PVP ensures that the Ag_m^{m+}-PVP complex rather than single Ag^+ ion is reduced [23]. And some references reported that PVP not only served as the stabilizer but also as a weaker reducing agent to reduce silver ions to silver under microwave irradiation compared with n-dodecanethiol, AOT, and poly(N-methyl acrylamide) (PMA) [55]. Fig. 3 shows a simple schematic illustration of the protective mechanism of PVP in the synthesis of silver nanoparticles through electrochemical reduction.

Nan *et al.* [48] synthesized new chainlike and dendritic silver nanostructures with fractal features by a simple solvothermal method using PVP as an adsorption agent and architecture soft template. They demonstrated that the morphology of the silver nanostructures changed with prolonging reaction duration. Fig. 4 shows a typical schematic process.

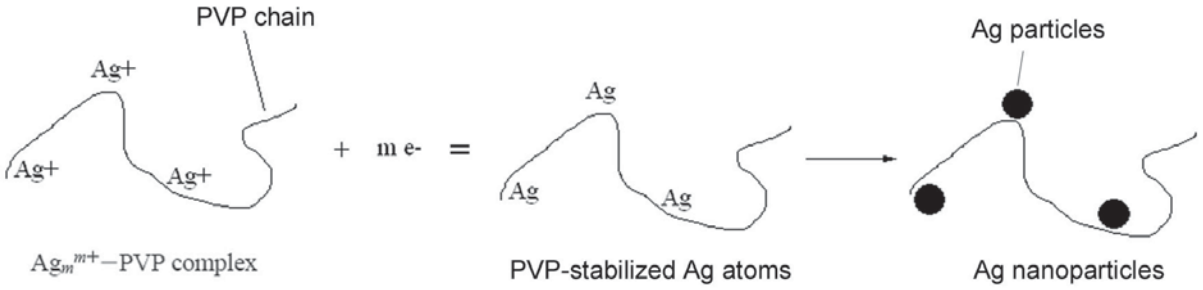

Fig. 3. Schematic illustration of the protective mechanism of PVP in the electrochemical synthesis of silver nanoparticles. Reprinted with permission from [23], copyright 2003, American Chemical Society.

Silver nanoparticles formed by the chemical reduction in ethylene glycol (reductant) solution, and then PVP adsorbed on the surfaces of the silver nanoparticles to induce the formation of the chainlike structures with fractal trees. With the necks between continuous silver particles in the branches of the chainlike structures disappeared in the growth process of crystals, the dendritic silver nanostructures formed gradually. The PVP herein play a role as an adsorption agent and architecture soft template to protect the nanoparticles in solution and keep the chainlike growth, respectively. When the concentration of the silver ions and reducer greatly decrease in the later period, the growth is drove by decrease of surface energy that causes the disappearance of necks and the formation of dendritic structures.

On the basis of the mechanisms expounded in the foregoing, several phenomenons observed in the experiments of the silver nanostructures synthesis could be explained logically. It has been reported that the morphology or the aspect ratio of the silver nanostructures using this method was highly dependent on the concentration of PVP (or the molar ratio between PVP and silver ions) [42]. With the high concentration of PVP or molar ratio of PVP to silver ions, only silver nanospheres were obtained as the product, with the low concentration or molar ratio, the silver nanowires can be generated, but with the relatively low concentration or molar ratio, needlelike structures with rough surfaces and sometimes even dendritic structures whose size often bigger than 1 μm were produced. It can be explained that a high concentration of PVP was not favorable for the formation of MTPs and might lead to cover the entire surfaces of an MTP, including the twin boundaries, so the selectivity in interaction between PVP and various crystallographic planes was lost. But a relatively low concentration of PVP was not able to form a continuous layer to passivate the side surfaces of nanowire completely, resulting in loose control over the growth of silver nanostructures in the lateral directions. The influence of the temperature of reaction might also be explained as the twin boundaries of MTPs melted slightly at relatively high

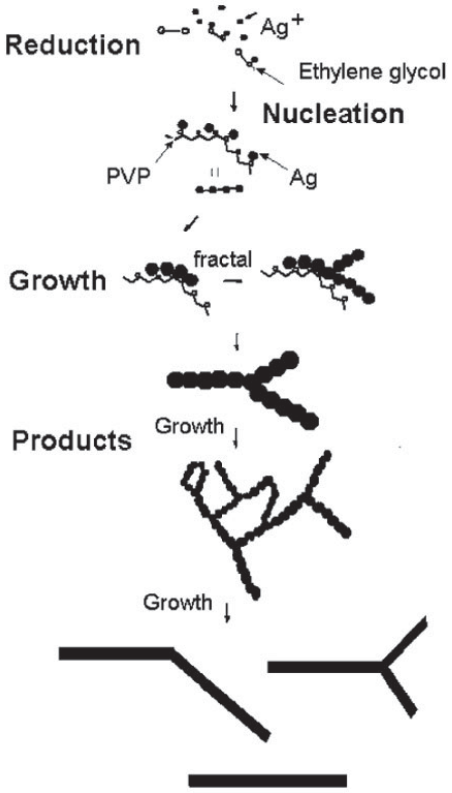

Fig. 4. Schematic illustration of the growth process of Ag chainlike and dendritic nanostructures. Reprinted with permission from [48], copyright 2003, American Chemical Society.

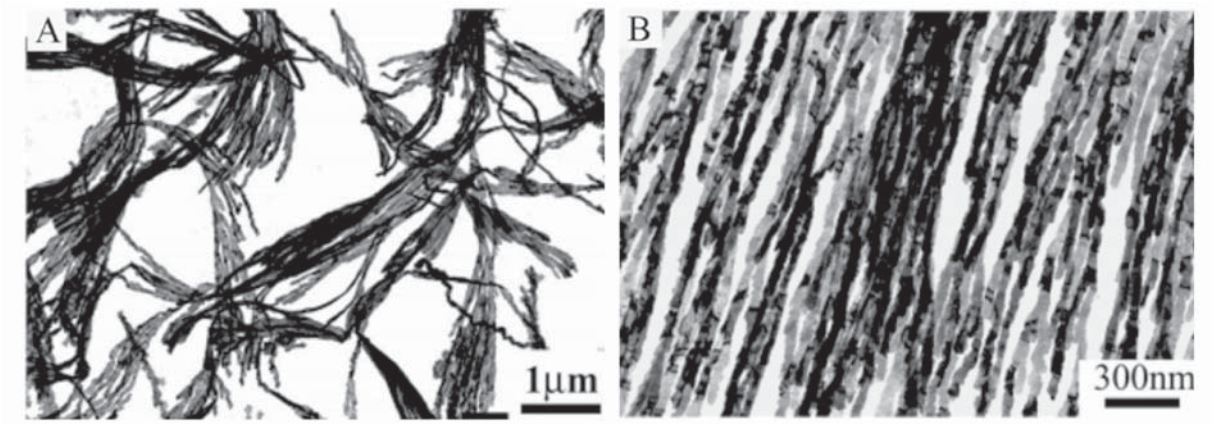

Fig. 5. TEM images of Ag nanowires constituting thin films. Reprinted with permission from [49], copyright 2004, American Chemical Society.

temperature act as intermediate phases to facilitate the transport of silver atoms from the solution phase to the growing surface.

Silver nanowire is the focus of many researches because of its inimitable characters and wider applied potential. Xia and Yang have reviewed this field very well [16], but there are still many problems should be studied and resolved. Lately, Qi *et al.* have prepared novel silver nanowires thin films on glass wall via mild chemical reduction in presence of poly(methacrylic acid) (PMAA) at ambient temperature [49]. Fig. 5 shows that the nanowires constituting thin film superstructures are longer than 10 mm, with the diameters from 30 to 40 nm. A possible growth mechanism is suggested: the glass wall is negatively when the pH is about 3.6 (typical synthesis condition), and it could preferentially adsorb the silver irons to form the heterogeneous nucleation sites for the anisotropic growth of bundles of silver nanowires under the protection of PMAA. Herein, the PMAA is considered to inhibit the nucleation and growth of silver crystal in the solution and act as efficient capping reagent to kinetically control the growth rates of different facets of the silver seeds on the glass wall to keep anisotropic growth and finally assemble to thin film superstructures.

In addition to the silver nanowires, other sturctures like cube, disk, hollow tube or box, triangular, prism, dendritic and etc have been also obtained. Xia *et al.* [50] have demonstrated a method to synthesize the silver nanocubes by reducing silver nitrate with ethylene glycol in the presence of poly(vinyl pyrrolidone) (PVP). These cubes were single crystals with a mean edge length of 175 nm, and were characterized by a slightly truncated shape bounded by {100}, {110}, and {111} facets (as shown in Fig. 6). It is possible to tune the size of silver nanocubes by controlling the experimental conditions like the concentration of $AgNO_3$, and the molar ratio between the PVP and $AgNO_3$, the temperature and the growth time. The selective adsorption of PVP on various facets of nanocubes is considered as the key in determining the product morphology. These silver nanocubes can be used to generate the hollow gold nanoboxs.

Pilent *et al.* [17] have synthesized silver nanodisks by reducing the silver di(2-ethylhexyl)sulfosuccinate (Ag(AOT)) with hydrazine in the presence of dodecanethiol used as capping reagent in the reverse micelles solution. This silver nanodisk (as shown in Fig. 7) is a strongly diffracting single crystal with highly anisotropic optical properties. The absorption spectrum of nanocrystals depends on the shape or aspect ratio of nanocrystals can also confirm the formation of silver nanodisks. However, the possible mechanism of the crystal growth was not provided.

Chen *et al.* [18] demonstrated a simple way to generate silver nanoplates with thickness of 20-30 nm and size of 40-300 nm (as shown in Fig. 8A) via chemical reduction in the presence of cetyltrimethylmmonium bromide (CTAB) and silver seeds in aqueous. When the concentration of CTAB is appropriate, the heads of molecules can self-assemble to form a network superstructure, and it plays a role as soft template to induct the anisotropic growth of the silver crystal seeds to nanoplates. This mechanism is similar to the one of polyol process [22], and the adsorptions of CTAB molecules on different faces of crystal nanoplates are distinct.

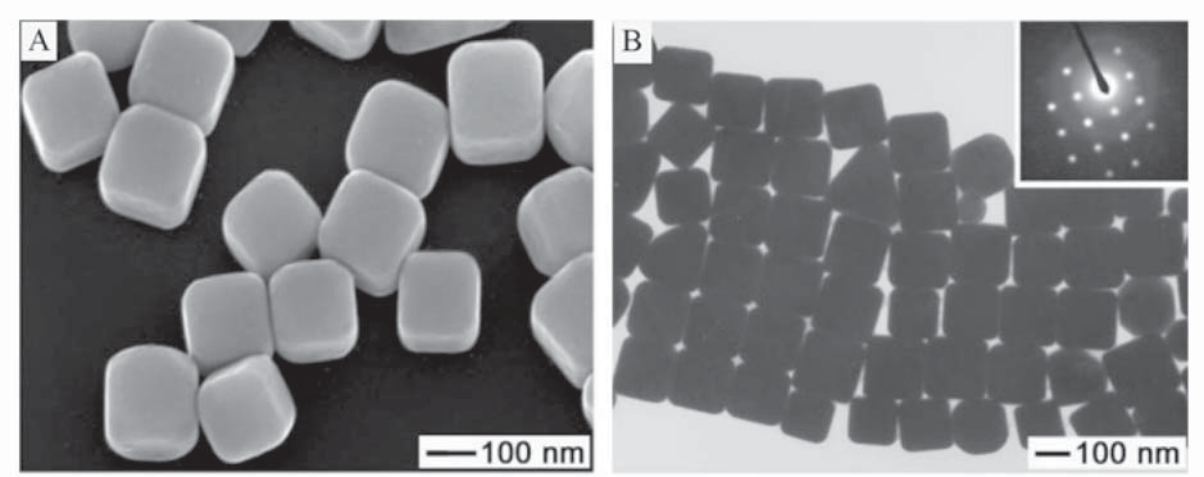

Fig. 6. (A) SEM image (left) and (B) TEM image of silver nanocubes, the inset shows the diffraction pattern recorded by aligning the electron beam perpendicular to one of the square facets of an individual nanocube. Reproduced with permission from [50], copyright 2002, AAAS.

Herein, the bromine anions and silver seeds are indispensable to formation of nanoplates, the bromine anions of CTAB react with silver ions partially to form silver bromine particles that contact with silver seeds prepared (as shown in Fig. 8B), alone with the catalytic reduction of the seeds adsorbed on the (111) face regulated by CTAB molecules, the final products completed.

Dendritic silver supermolecular nanostructures have been synthesized via a chemical reduction in the presence of PVP several years ago [51]. Wang *et al.* [52] reported a new method to synthesize the silver dendritic nanostructures protected by tetrathiafulvalene (TTF) via reduction of silver ions with TTF in acetonitrile under the condition of the molar ratio of TTF to $AgNO_3$ below 1.8. TTF acts as reducing agent (electron donors) and the oxidized TTF acts as stabilizer as it holds a positive charge to interact with the surface of the silver dendrites through electrostatic force (as shown in Fig. 9B).

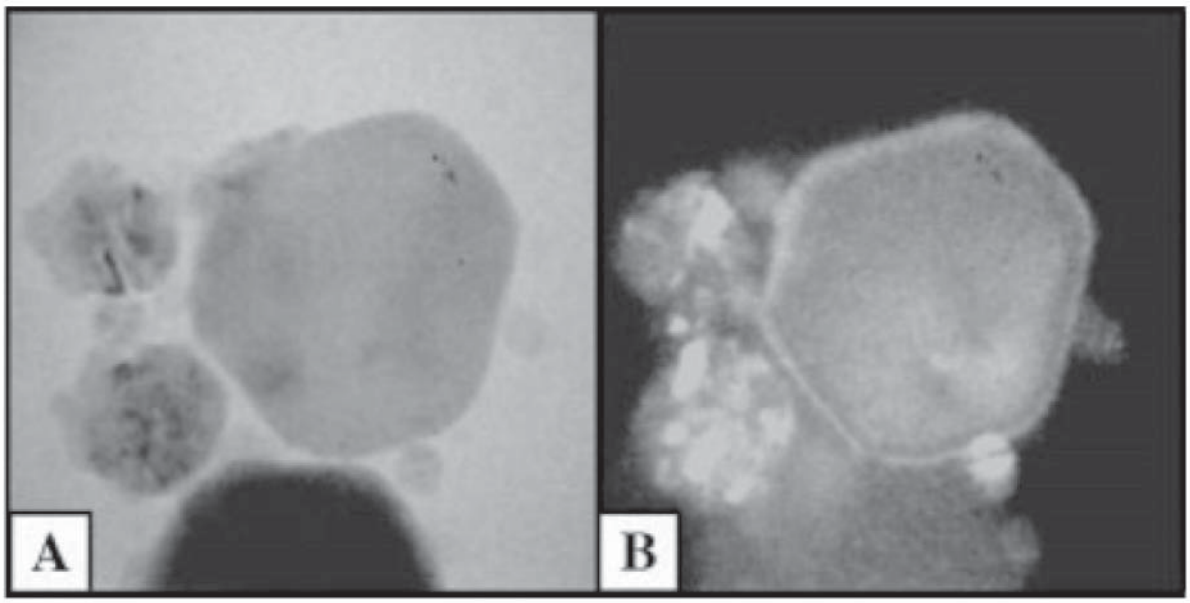

Fig. 7. (A) A bright-field TEM image of a mixture of spheres and nanodisks. (B) A dark-field TEM image of a mixture of spheres and nanodisks. Reprinted from [17] with permission, copyright 2002, John Wiley & Sons, Inc.

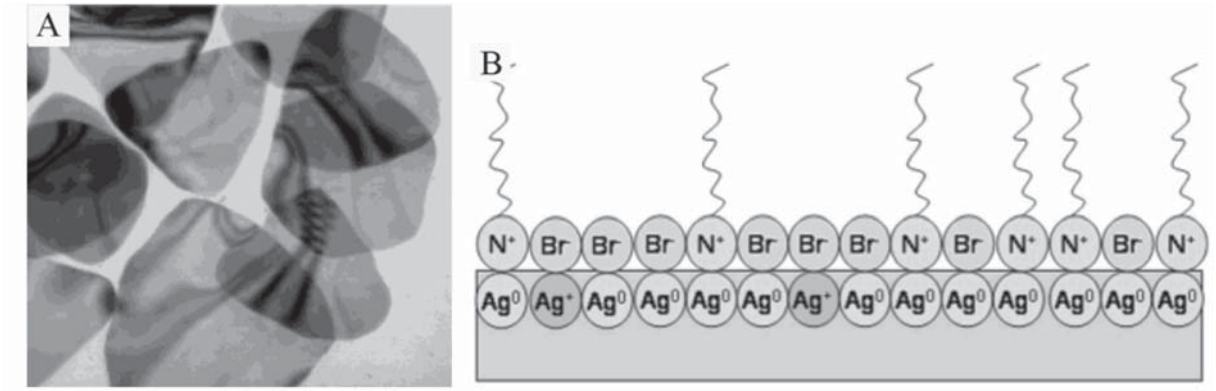

Fig. 8. (A) A TEM image of the silver nanoplates with size about 283 nm. (B) Schematic illustration of self-assembled layer of CTAB molecules on silver plate surface. Reprinted with permission from [18], copyright 2004, American Chemical Society.

The tendency to crystallize and diminish charge of the oxidized TTF makes it is a weaker stabilizer than PVP, however this tendency facilitates the formation of the well-defined silver dendritic nanostructures as the growth might occur in the interspaces of the resulting crystals of TTF [53]. When the molar ratio of TTF to $AgNO_3$ above 1.8, rodlike crystals along with the spherical particles were obtained after 21 h of reaction as the TTF-based crystallite grew rapidly by π-stacks of TTF radical cations in the direction of the *c*-axis [54]. Dendritic structures with the diameter of 1.32 ± 0.24 μm appeared after stirring the reaction mixture for 6 h and the size of the dendrites gradually increased with an increase of the reaction time due to the increased amount of generated radical cations of TTF and metallic silvers in the solution (as shown in Fig. 9A).

Qian *et al.* [55] investigated the influence of the different solvent on the morphology of silver nanoparticles by a soft solution approach under microwave irradiation from a solution of silver nitrate in the presence of poly(N-vinyl- 2-pyrrolidone) (PVP) without any other reducing agent. They prepared the silver nanoparticles in pyridine, ethanol, DMF, NMP and discovered that in the DMF obtained regular

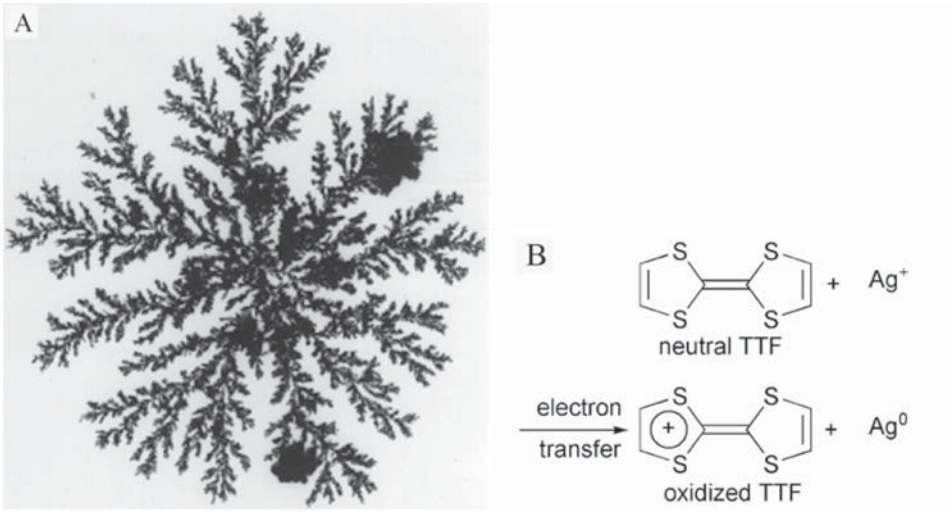

Fig. 9. (A) TEM image of a silver dendritic nanostructure observed after 21 h reaction, white bar =200 nm. (B) Schematic illustration of reaction mechanism, [52]. Reproduced by permission of The Royal Society of Chemistry.

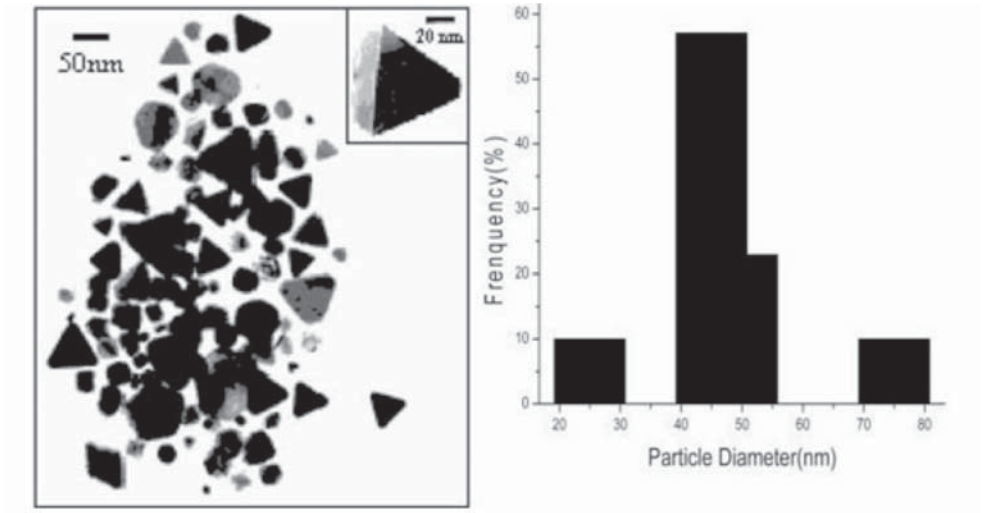

Fig. 10. TEM images (left), inset showed single silver nanoprism and size distribution histograms of silver nanoparticles in DMF solvents (right), [55]. Reproduced by permission of The Royal Society of Chemistry.

geometrical shape, most of which are triangular (edge length about 50–100 nm) or truncated triangular single crystal nanoprisms(as shown in Fig. 10). The dielectric properties and the boiling points of the solvents had an important effect on the crystallinity of the silver nanoparticles. Higher boiling point solvents were advantageous to the higher crystallinity of the silver nanoparticles. The exact mechanism for the formation of different shape and morphology of the silver particles in different solvents is still unclear, maybe relate to the reducing ability of DMF demonstrated by Pastoriza-Santos and Liz-Marzan [56].

Mirkin *et al.* [57] have demonstratered a photoinduced method to convert large quantities of silver nanospheres into single crystal triangular nanoprisms. Silver ions are reduced by $NaBH_4$ in the presence of trisodium citrate and bis(*p*-sulfonatophenyl) phenylphosphine dihydrate dipotassium salt solution (BSPP) as stabilizing agents to prepare the silver nanospheres, and then irradiated with a conventional 40-W fluorescent light. After 70 hours more than 99% of the initial spheres are converted to nanoprisms with the edge length about 100 nm and the thickness about 15.6 nm (as shown in Fig. 11). The conversion can be initiated by light at wavelengths between 350 to 700 nm, but does not be take place in irradiation with near-infrared light (>700 nm) or in the dark. The process of this preparation can be classified into three distinctive stages: induction, growth, and termination. In the induction period extremely small spherical silver nanoclusters (2 to 4 nm) are formed by the photoinduced fragmentation [58], in the growth period the small nanoprisms (5 to 10 nm edge lengths) act as seeds and grow into larger nanoprisms with the consumption of nanoparticles, with the exhaustion of the spherical nanoparticles and small nanoclusters, and the reaction terminates finally. Further research has demonstrated that using wavelength to control the size of nanoprisms is a good method. It is obtained a bimodal distribution of the sizes of nanoprisms with the smaller particles and the larger particle having average edge lengths of 70 nm and 150 nm respectively under the light irradiation at wavelengths between 500 to 700 nm [59].

Murphy *et al.* [60] reported a method to synthesis silver nanowires with clean surfaces in absent of surfactant, polymer as stabilizer or seed as initiating agent in the alkali solution without purification, and the final nanowires yield is high with relatively few byproducts like spherical nanoparticle. In this synthesis, silver ions is reduced by trisodium citrate, sodium hydroxide is added as pH modifying agent. The citrate herein is performing not only the strong complexing reagent to the silver ion, but also responsible reduction to silver metal and as a capping agent to the nanometal. The equilibrium constant for citrate binding to certain crystal faces of silver may begin to differ with the elevated temperature, leading to selective loss of citrate on certain crystal faces and allowing for the nanoparticles to

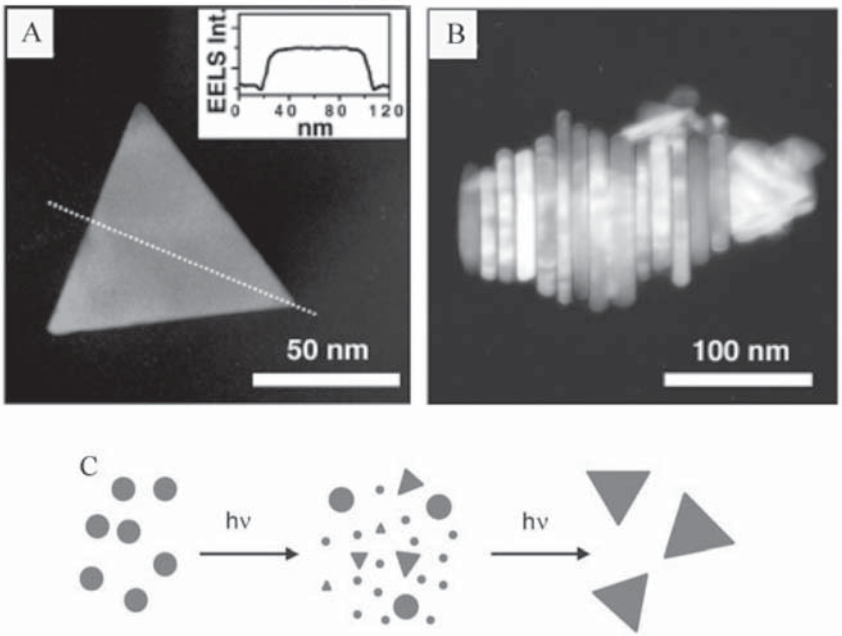

Fig. 11. (A) A electron energy loss spectroscopy analysis (EELS) image of the flat top morphology of the Ag nanoprisms, inset shows the EELS intensity over the line scan (dotted line through triangle axis). (B) A TEM image of stacks Ag nanoprisms. (C) Schematic illustration of reaction mechanism. Reproduced with permission from [57], copyright 2001, AAAS.

grow along only one axis. The quantity of NaOH can change the complexing of the citrate and is considered as an important factor in determining the morphology of the final product, a small amount of NaOH favors the citrate to be a weaker complexing agent and allows the nanoparticles grow into sinter together and formed larger agglomerates of silver, while a large amount of NaOH favors the complexing level of hydroxide to be stronger than citrate and allowed the formation of irregularly shaped particles.

2.2. Chemical preparation of special-shaped gold nanomaterials

Gold nanomaterial is the most stable metal nanomaterial with potential application involving electronics, magnetics, optics, materials, catalysis and biology, so it is considered as the key material and building block in future [20]. Many conventional methods of preparation of silver nanomaterials can also be used to synthesis of gold nanomaterials.

Chemical reduction of gold metal salts in aqueous medium or organic solvents with linear polymers as capping agents such as ploy(vinylpyrrolidone) (PVP) and poly(vinyl alcohol) (PVA) has been used to generate shape-controlled gold metal nanoparticles. The mechanism of this preparation is similar to the mechanism of preparation of the PVP-stabilized silver nanoparticles [42]. Zhou *et al.* [61] present a simple chemical protection–reduction technique for producing shape-controlled gold nanostructures at room temperature, using $KAu(CN)_2$ as the gold source and PVP as the capping agent. The reducing agent such as ascorbic acid (AA), oxalic acid, or hydrazine mixed with the capping agent prior to addition to the solution. The molar ratio of AA/PVP in experimental conditions is a crucial factor. The nanoparticles are spherical at molar ratios <3, while they adopt cubic shapes at ratios in the range 4–6. If the molar ratio of AA/PVP is >7, the Au nanoparticles will self-assemble into dendrite structures (as shown in Fig.12).

Metal nanostructures with hollow interiors have been shown to exhibit a range of interesting properties superior to their solid counterparts [62-64] such as relatively low densities [65], plasmonic properties completely different from those of solid ones [66-67]. In early instance, Au_2S/Au core-shell

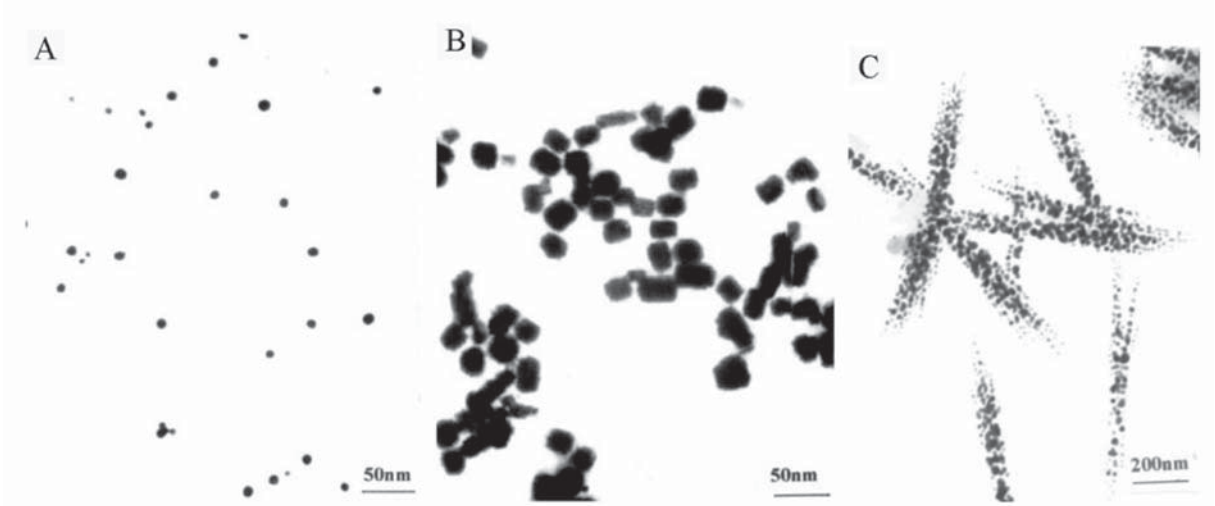

Fig. 12. TEM images of Au nanoparticles synthesized at various AA/PVP (AA=1.4 mmol, $KAu(CN)_2$ = 0.007 mmol), (A) AA/PVP = 2, spherical, (B) AA/PVP = 4, cubic, (C) AA/PVP = 10, dendrite structures, [61]. Reproduced by permission of The Royal Society of Chemistry.

nanostructures with diameters of ~50 nm were synthesized by mixing aqueous solutions of Na_2S and $HAuCl_4$ with appropriate molar ratios [68]. Formation of gold shells on the surfaces of silica nanoparticles through nanoscale self-assembly [69] and layer-by-layer adsorption of polyelectrolytes and charged gold colloids to the surface of the template particle to build a shell structure [70] are other two early methods. But the metal nanoshells synthesized by all of these methods are polycrystalline in structure. Xia *et al.* [50] developed a simple and convenient route to get metal nanostructures with hollow interiors and highly crystalline walls by the galvanic replacement reaction between the more reactive metal nanoparticles and the desired metal ions solution. Single crystalline hollow structures of metals whose void sizes are determined by the diameters of templates can also be obtained when the templates are single crystals. With gold as an example, silver nanostructures suspended in solution act as reductants of $HAuCl_4$, and the elemental gold produced in this reaction is confined to the vicinity of the template surface. These gold shells final obtained have the morphology similar to that of the silver templates, with their void sizes mainly determined by the dimensions of templates [72-73]. Fig. 13A shows a TEM image of the silver nanoparticles that were used as templates. Fig. 13B shows a TEM image of the result of these silver nanoparticles after they have completely reacted with the aqueous $HAuCl_4$ solution. The center portion of each particle was lighter than its edge, indicating the formation of a shell-type hollow nanostructure. Fig. 13D shows a TEM image of gold nanoboxes self-assembled into a close-packed 2D array during sample preparation, illustrating the high symmetry of this polyhedral hollow nanoparticle. Gold nanotubes with a uniform wall thickness agreed well with the value in theory formed by templating against bicrystalline silver nanowires [22,72] (as shown in Figs. 13C and 13E).

Murphy *et al.* [74] prepared uniformly shaped gold nanorods with high aspect ratio by a seeding growth process in the reduction of $HAuCl_4$ with borohydride, in the presence of CTAB as an aqueous rodlike miceller template and preformed gold nanoparticles as growth seeds. The aspect ratio of nanorods can be carefully controlled by proper adjustment of the growth conditions. Concentrated CTAB has a tendency to form elongated rodlike micellar structures [76], so that nanorods yield decreased when this micellar template (CTAB) was absent. Herein, CTAB can be replaced by polystyrene or silica. Polystyrene coating was accomplished by the emulsion polymerization of styrene in the presence of CTAB-coated gold nanorods as seeds, and ammonium persulfate was added as the initiator. Silica coating was accomplished by adding (3-mercaptopropyl)-trimethoxysilane (MPTMS) solution into the CTAB-coated gold nanorods solution, freshly prepared aqueous sodium silicate solution was added in sequence. The different coating reagents resulted in a

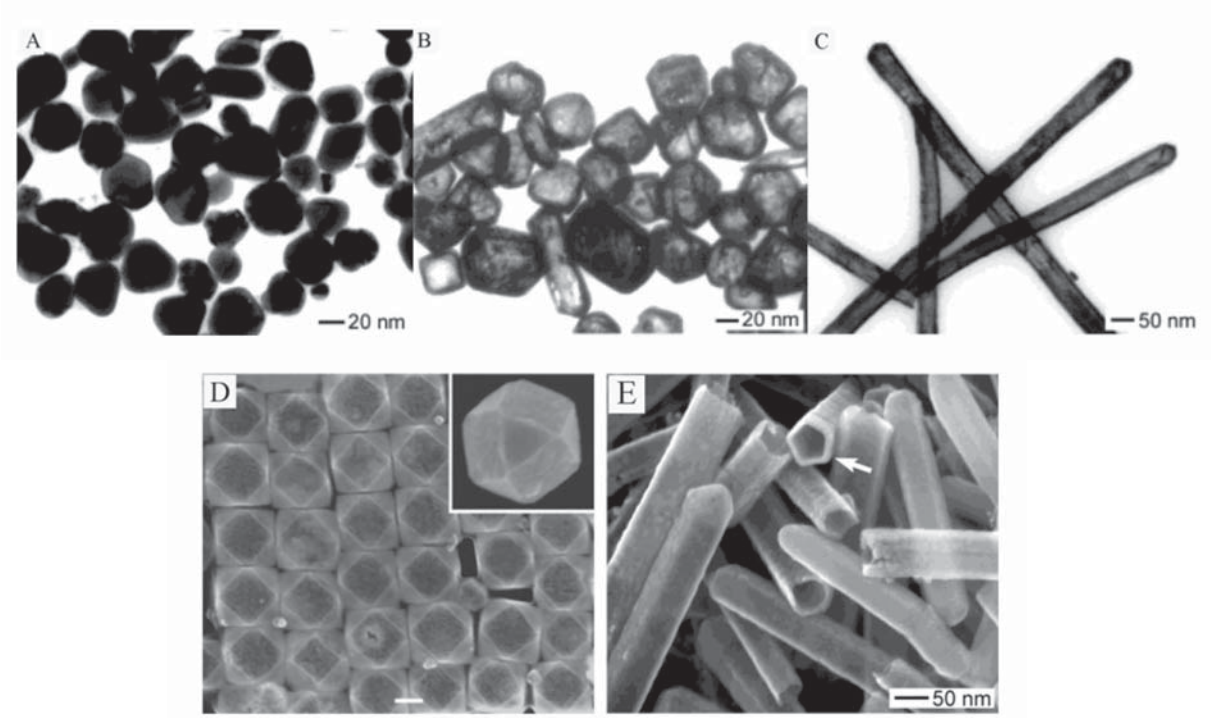

Fig. 13. (A,B,C) The TEM images of silver nanoparticles templates and gold nanoshells formed by replacement reaction. Reprinted with permission from [72], copyright 2002, American Chemical Society. (D) A TEM image of gold nanoboxes prepared by reacting silver nanocubes with an aqueous $HAuCl_4$ solution. Reprinted with permission from [50], copyright 2002, American Chemical Society. (E) A SEM image of gold nanotubes that had been broken to show their cross sections [22]. Reprinted with permission from [22], copyright 2003, American Chemical Society.

modification of the optical properties of the gold nanorods [77]. Fig. 14A shows the TEM image of 18 aspect radio gold nanorods with short axes about 16±3 nm. Fig. 14B indicates that the polystyrene appears as a uniform white layer around the gold nanorods. Fig. 14C indicates that the silica appears as a thick layer around the gold nanorods without staining. If using KCN to dissolve the gold core, the hollow polystyrene and silica nanotubes will be left. However, the yield of gold nanorods synthesized via above method is low, ~ 4%, fortunately, an improved method to synthesis of these high-aspect-ratio gold nanorods has been developed [78]. This method involved a three-step seed-mediated growth process. Firstly, 4 nm gold nanoparticles are produced by the conventional method at pH 2.8, secondly, these nanoparticles are added to a growth solution containing CTAB (capping agent), HAuCl4, and ascorbic acid (reductant), thirdly, and it is the key step, appropriate sodium hydroxide is added to the solution, then the pH raises to 3.5, as a result, the yield of gold nanorods increases to ~ 90%. Obviously, an increase in pH from 2.8 to 3.5 represents a significant increase in the fraction of ascorbrate that is demonstrated as a more effective reductant in the presence of CTAB [79], and it is the key of the improvement of nanorods yield. Recently, they obtained short gold nanorods ranging in length from 20 to 100 nm with the aspect ratio from 2 to 4 in high yield via similar method in the presence of CTAB and silver ions [80]. These gold nanorods are considered as potential candidates for sensor applications.

Chen *et al.* [81] reported the first example of the branched (tripod and tetrapod) gold nanocrystals via a chemical reduction in the presence of CTAB in aqueous solution at room temperature. Fig. 15 shows possible growth processes of tripod and tetrapod nanocrystals, however, not all of the particles can grow to form these multangular crystals, more than 80% stop in the stepwise pod extrusion process. CTAB plays the role as stabilizer, if strong adsorption occurred on the six {100} planes, the tetrapod nanocrystals were formed, if strong adsorp-

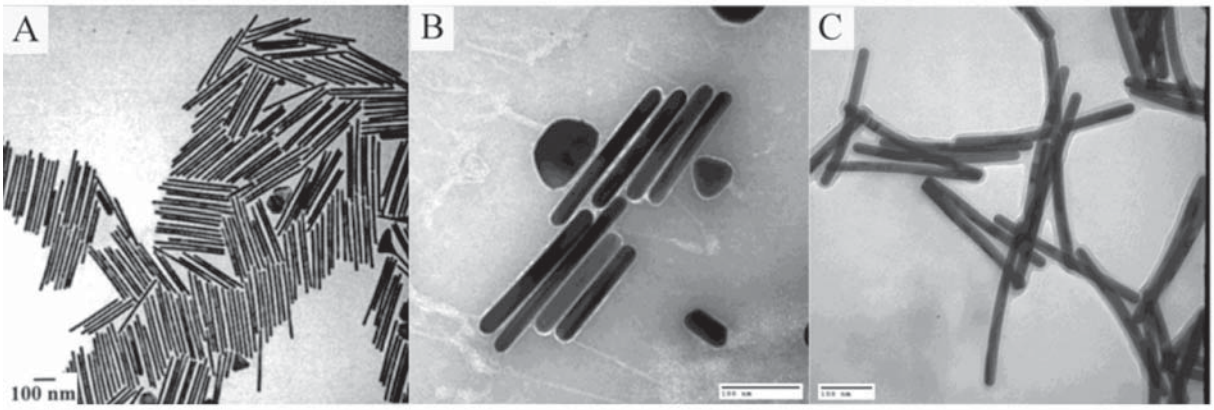

Fig. 14. (A) A TEM image of 18 aspect ratio gold nanorods coated with CTAB [74]. Reprinted with permission from [74], copyright 2001, American Chemical Society. (B) A TEM image of 13 aspect ratio gold nanorods coated with polystyrene. (C) A TEM image of 13 aspect ratio gold nanorods coated with silica. Reprinted with permission from [77], copyright 2001, American Chemical Society.

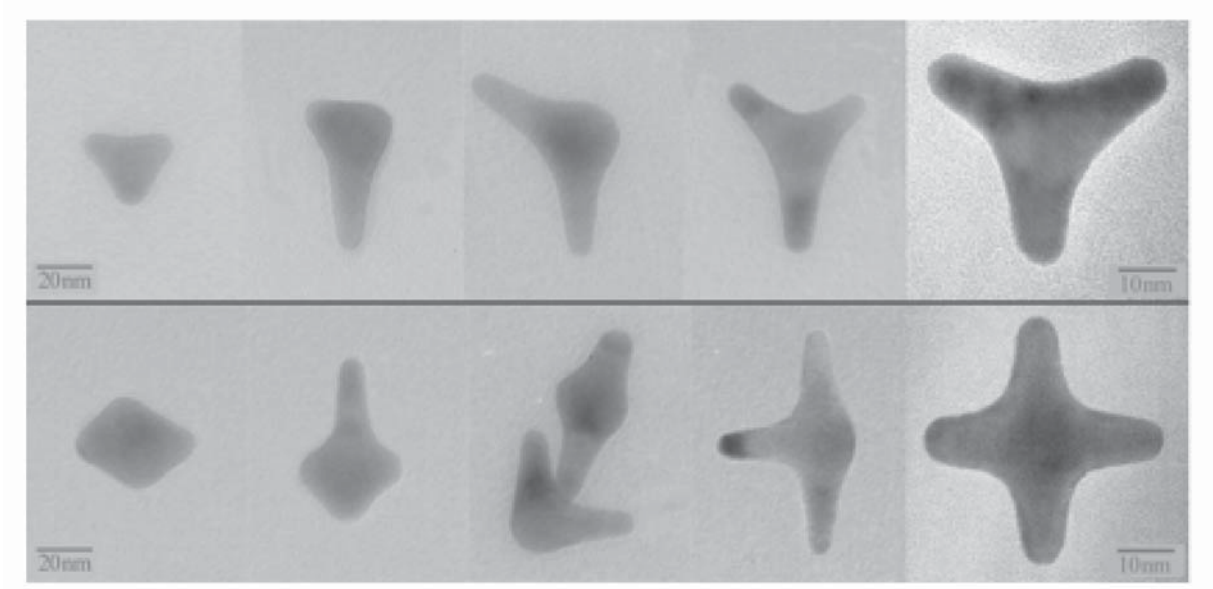

Fig. 15. TEM images of different developing stages of pod growth toward tripod and tetrapod gold nanocrystals. Reprinted with permission from [81], copyright 2003, American Chemical Society.

tion occurred on the {110} and {111} planes synchronously, the tripod nanocrystals were formed, the result of element analysis of branched crystals demonstrated that the CTAB molecules adsorb on the surfaces of these crystals.

2.3. Chemical preparation of special-shaped copper nanomaterials

Copper has very high electrical conductivity in the common bulk metals and has a wide range of commercial applications as its cheap price in metal materials. The physical and chemical properties of special-shaped copper nanomaterials are superior compared with bulk copper, so their applications can be expected to bring in many new fields. However it is a great challenge to prepare special-shaped copper nanomaterials through chemical reduction in soft solution as the chemical property of copper is more active than silver and gold.

Qian *et al.* [82] reported a simple and effective soft template approach to synthesis the single crystalline copper nanowires (as shown in Fig. 16) with average diameters of ~85 nm and lengths of several tens of micrometers by a complex-surfactant- assisted hydrothermal reduction at a low temperature.

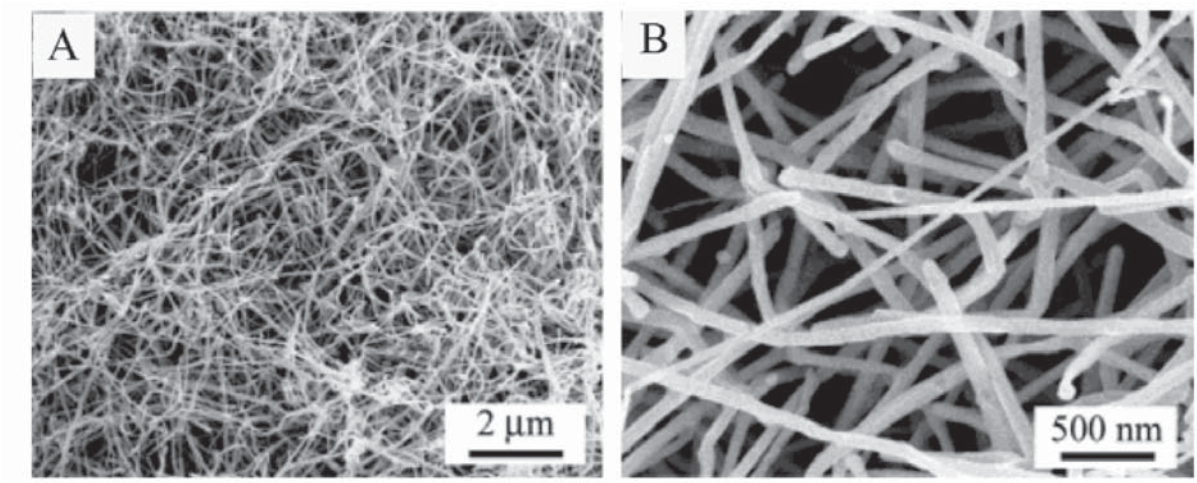

Fig. 16. FESEM images of obtained copper nanowires (A) low-magnification view, (B) high-magnification view. Reprinted with permission from [82], copyright 2003, American Chemical Society.

In a typical process, copper (II)-glycerol complexes blended of bluestone and glycerol were reduced by sodium phosphate in the presence of surfactant sodium dodecyl benzenesulfonate (SDBS) at 120 °C, and uniformly copper nanowires obtained after some treatments. In this controllable synthesis, SDBS played as capping agent to prevent the aggregation of copper nanoparticles produced in the initial stage of the growth and induce the anisotropic growth of copper nanowires through selectively adsorbing on various facets. Interestingly the SDBS cannot be replaced by other common surfactants such as SDS, PVP, CTAB or no nanowires observed.

Xie *et al.* [83] have synthesized junction structures of copper nanorods with a high yield and uniform morphology by a novel soft templates consisted of poly(ethylene glycol) (PEG) and CTAB. In a typical experiment, appropriate concentrations of PEG, CTAB, and CuCl2·2H2O mixed together and rested for 4 hours in favor of the interaction of copper ions with the supermolecule structures generated by the combination of PEG and CTAB, then the solution was heated up to 100 °C, mixing with excess potassium borohydride solution (reductant) quickly, and then kept reacting for 3 hours. Fig. 17 shows the single crystal nanorods radiated from the junctions have diameters from 40 to 80 nm, and these start-shaped junctions have uniform sizes. The growth mechanism can be interpreted by the astriction of supermolecule structures composed of polymer coil and rod-shaped micelles. It is presumed that the copper cores and nanorods formed simultaneously and grew rapidly. These junctions are expected to apply in fabrication of optoelectronic devices.

2.4. Chemical preparation of other special-shaped metal nanomaterials

Many kinds of special-shaped metal nanomaterials can be synthesized by chemical reduction, herein we review some interesting results reported recently.

The selenium nanowires prepared by various methods [84-86] can be used to synthesize other metal nanotubes like platinum nanotubes by surface treatment, and it is described that the selenium nanowires act as template in the soft solution to induce the formation of platinum nanostubes with complementary morphology via galvanic replacement reaction [87]. Though the morphology of the final platinum nanotubes are similar to the template of selenium nanowires, the thickness of the platinum nanotubes is defined by the redox reaction between Pt(II) salt and alcohol solvent (rather than the Se template). It is explained by a plausible coating process: galvanic reduction between Pt(II) salt and Se template occurred first in the initial time and continue until the surface of template covered completely, subsequently deposition of the Pt produced by the alcohol reduction induce the bodiness of the wall of Pt nanotube. The Se template can be dissolved in hydrazine monohydrate finally. Fig. 18A shows the TEM image (left) and SEM image (right) of trigonal platinum nanotubes prepared by coating for 18 hours. Fig. 18B shows the TEM image of platinum nanotube contained the selenium nanowire that was prepared for 3 days, the black portion is the Pt nanotube and the gray portion is the Se nanowire core generated via removal the Pt sheath

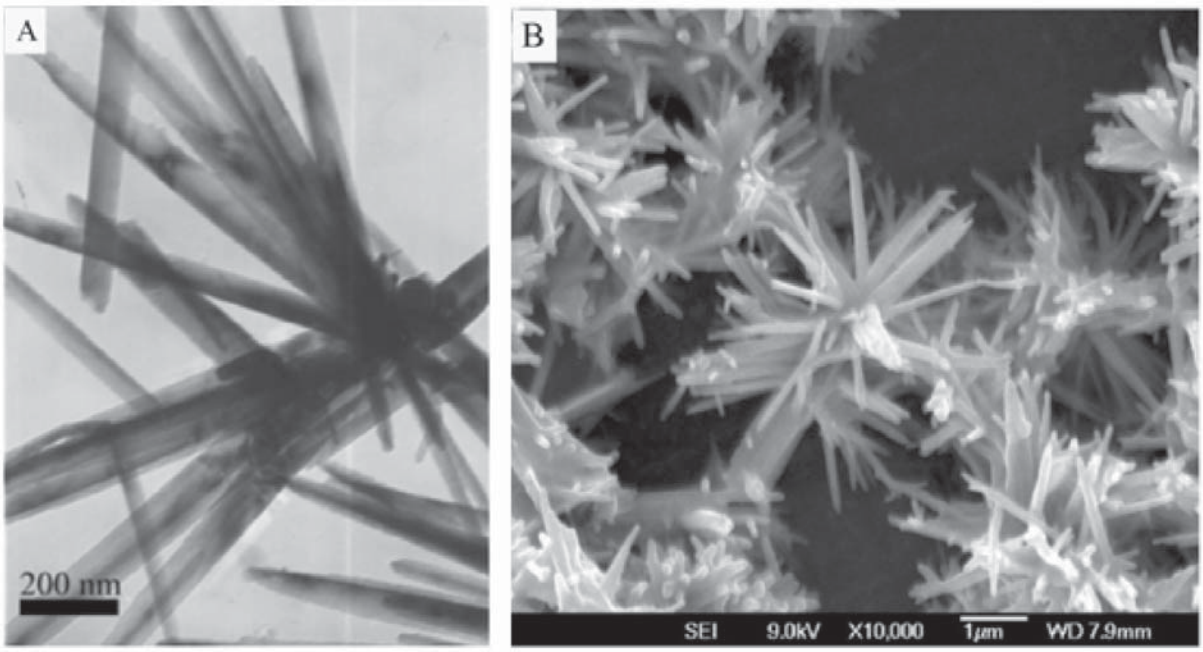

Fig. 17. TEM (A) and FESEM (B) image of the uniform junction structures of single crystal copper nanorods. Reprinted from [83], copyright (2003), with permission from Elsevier.

by sonication, the inset electron diffraction pattern of the exposed Se core indicates that no structural change was involved for the Se template during Pt coating.

Xia *et al.* [88] have demonstrated to product single crystalline lead nanowires with uniform diameters of 50-90 nm and lengths up to several millimeters (as shown in Fig. 20C) by a simple route include thermal decomposition and polyol process in the presence of PVP under N_2 protection. The growth mechanism is supposed that involve the solution-liquid-solid mechanism and Ostwald ripening mechanism. In a type growth of the silver crystals, the elemental lead is formed firstly by the thermal decomposition of lead acetate with the help of ethylene glycol to reduce the temperature required, then these lead atoms grow into nanoparticles through a homogeneous nucleation process with the protec-

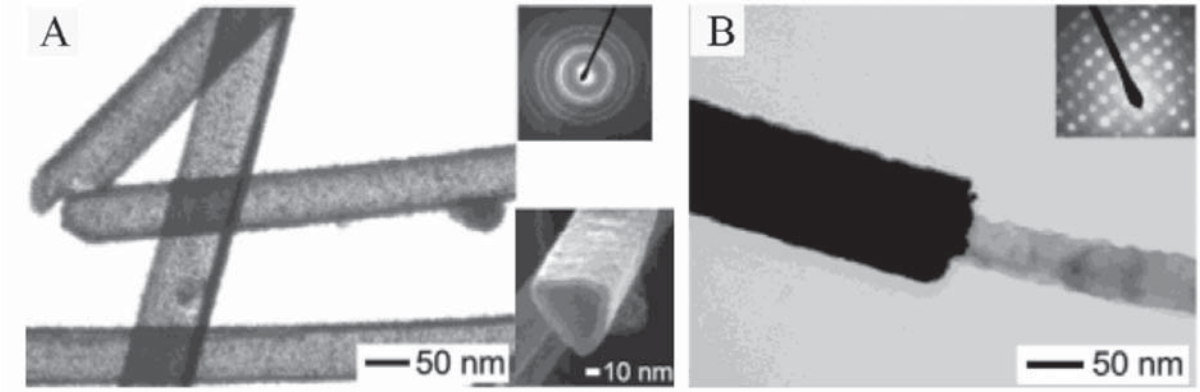

Fig. 18. (A) TEM image (left) and SEM image (right) of Pt nanotubes, the insert shows the electron diffraction pattern. (B) A TEM image of Pt nanotube contained Se nanowire, the inset shows an electron diffraction pattern taken from the exposed Se core. Reprinted with permission from [87], copyright 2003, American Chemical Society.

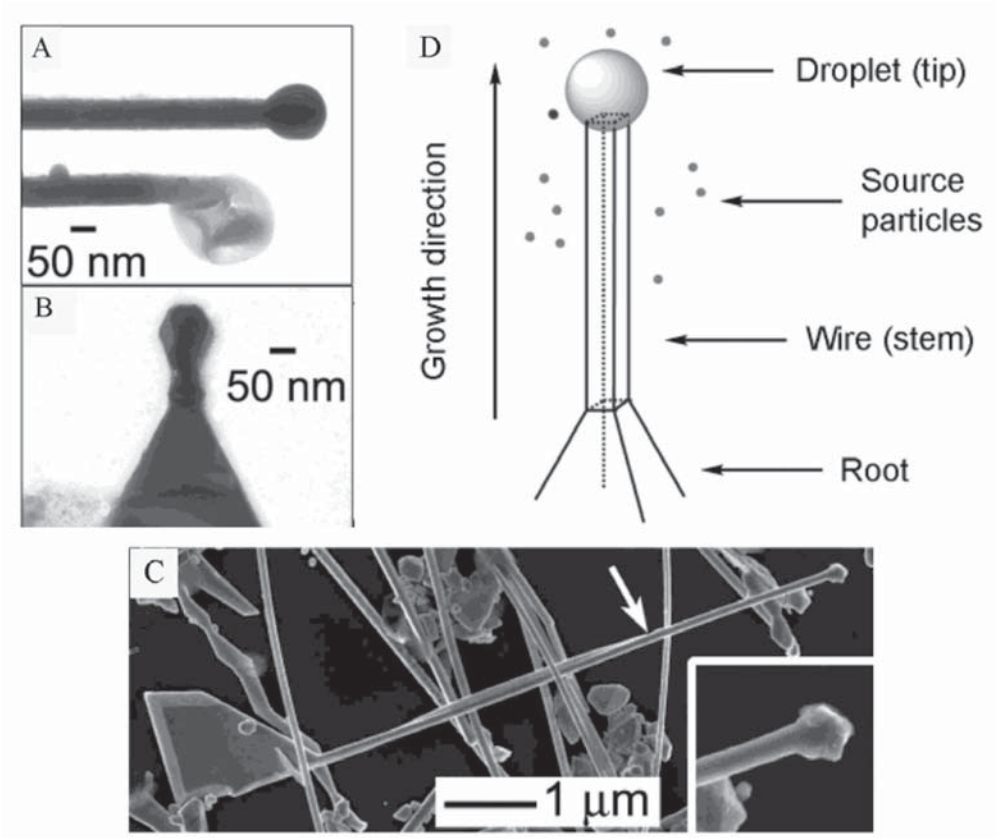

Fig. 19. (A) A TEM image of two nanowires whose tips are terminated in droplets. (B) A TEM image of growing nanowire in the early stage of growth, showing root, tip. (C) A SEM image of growing lead nanowire, showing root, tip and wire, the inset gives a magnified view of the tip. (D) Schematic illustration of the proposed mechanism for nanowire growth. Reprinted with permission from [88], copyright 2004, American Chemical Society.

tion of PVP, meanwhile some larger crystals with sizes of several micrometers are also formed, whose corners will be the site of further nucleation and growth of nanowires driven by Ostwald ripening. Normally, the nanowires start form the sharpest corners of the micrometer-sized root, the surface atoms on these corners are reactive to adsorb lead atoms from the melted nanoparticles around to form the liquid droplets eventually. When the sizes of the droplets have reached a critical value, the lead atoms will start to crystallize into solid at the interface between the droplet and the root, after more atoms adsorbed into the droplets via Ostwald ripening the lead nanowires are formed finally. Fig. 19 provides some evidential images and the schematic illustration of the proposed mechanism for nanowire growth.

Anisotropic magnetic nanoparticles like iron are expected to apply to ultrahighdensity magnetic storage devices because of shape anisotropy [89]. Many research groups have used $Fe(CO)_5$ as precursor to synthesize iron nanoparticles through chemical reduction, but the magnetization of these nanoparticles produced is depleted [90]. Chaudret *et al.* [91] have demonstrated the iron nanocubes generated via the decomposition of the iron-organic precursor $Fe[N(SiMe_3)_2]_2$ in the presence of a long-chain acid(oleic acid, OA or hexadecylamonium chloride, HDAC) and a long-chain amine(hexadecylamine, HDA) under H_2 atmosphere exhibit magnetic properties that match those of bulk iron. These nanocubes with edges of about 7 nm (as shown in Fig. 20) can be incorporated into larger crystalline superlattices, in which the interparticle spacing is estimated at about 1.6 nm, and these spacing are supposed that the long-chain ligands adsorbed at the surfaces of nanocubes.

Dendrimer is considered as a novel chemical additive in the synthesis of metal nanomaterials via chemical reduction. However the recent reported

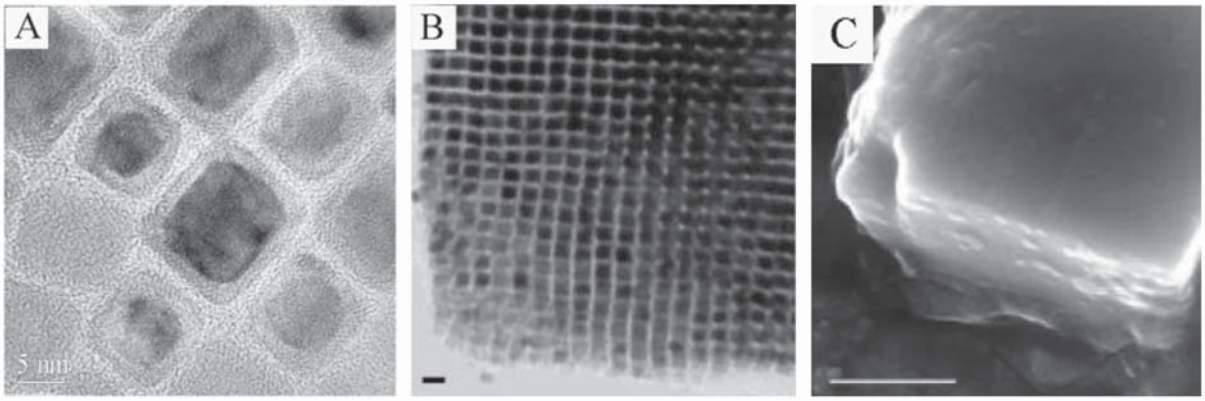

Fig. 20. (A) A HRTEM image of square nanocubes near the edge of a 3-D super lattice, white bar = 5 nm. (B) A TEM image of a 3-D superlattice, black bar = 10 nm. (C) A SEM image of a 3-D super lattice, white bar = 500 nm. Reproduced with permission from [91], copyright 2004, AAAS.

researches [92-98] seem to indicate that the dendrimer is a good encapsulation agent to produce monodisperse metal nanoparticles core-dendirmer shell structures, few reports refer to the chemical preparation of the special-shaped metal nanomaterials in the presence of dendrimer.

3. APPLICATION OF SPECIAL-SHAPED METAL NANOMATERIALS

Special-shaped metal nanometals have the undoubted advantage in the fabrication of nanodevice. These hold promise for the miniaturizing of electronics, optics, magnetics devices, chemistry, biomedicine sensor, miceoreactor and *etc.* Tao *et al.* [99] have studied molecular adsorption onto stable copper nanowires fabricated with an electrochemical method, and discovered that the conductance of nanowire is determined by the adsorption of organic molecules. Bartlett *et al.* [100] discovered that the electrochemical deposition of nanostructured metal films like palladium offers a promising approach to the fabrication of micromachined calorimetric gas sensors for combustible gases. The working mechanism of these metal nanoscaled sensor is presumed that the electrical property of nanometals is extremely sensitive to the adsorption of something on surfaces because of its high aspect ratio. However, there are still few reports on the applications of special-shaped metal nanomaterials, maybe it should be explore the enhanced or new physical and chemical properties of these nanomaterials to develop the potential advanced applications wider.

4. SUMMARY

Special-shaped metal nanomaterials have been prepared through chemical reduction in soft solution with mild conditions. Linear Polymers and surfactants are effective encapsulation or inducement to control anisotropic growth of metal crystal. Many reported elementary and feasible mechanisms of soft solution processing have been discussed, but exact mechanism still should be studied to explain more phenomena observed in experiments. Fabrication of nanosensors by special-shaped metal nanomaterials has also been reported. And it is expected that these special- shaped metal nanomaterials will applied to obtain more novel and attractive nanodevices in future.

REFERENCES

[1] I. A. Ovid'ko // *Science* **295** (2002) 2386.
[2] G. Schon and U. Simon // *Colloid Polym. Sci.* **273** (1995) 202.
[3] S. M. Bachilo, M. S. Strano, C. Kittrell, R. H. Hauge, R. E. Smalley and R. B. Weisman // *Science* **298** (2002) 2361.
[4] W. U. Huynh, J. J. Dittmer and A. P. Alivisatos // *Science* **295** (2002) 2425.
[5] M. S. Gudiksen, L. J. Lauhon, J. Wang, D. C. Smith and C. M. Lieber // *Nature* **415** (2002) 617.

[6] J M. Thomas // *Pure Appl. Chem.* **60** (1988) 1517.
[7] L. N. Lewis // *Chem. Rev.* **93** (1993) 2693.
[8] J. Kong, N. R. Franklin, C. Zhou, M. G. Chapline, S. Peng, K. Cho and H. Dai // *Science* **287** (2000) 622.
[9] M. Bruchez, M. Moronne, P. Gin, S. Weiss and A. P. Alivisatos // *Science* **281** (1998) 2013.
[10] W. C. W. Chan and S. M. Nie // *Science* **281** (1998) 2016.
[11] T. A. Taton, C. A. Mirkin and R. L. Letsinger // *Science* **289** (2000) 1757.
[12] S. R. Nicewarner-Pena, R. G. Freeman and B. D. Reiss // *Science* **294** (2001) 137.
[13] Y. Cui, Q. Wei, H. Park and M. Leiber // *Science* **293** (2001) 1289.
[14] J. Amblard, O. Platzer, J. Ridard and J. Belloni // *J. Phys. Chem. B* **96** (1992) 2341.
[15] Z. L. Wang // *Adv Mater.* **12** (2000) 1295.
[16] Y. Xia, D. Yang, Y. Sun, Y. Wu, B. Mayers, B. Gates, Y. Yin, F. Kim and H. Yan // *Adv. Mater.* **15** (2003) 353.
[17] M. Maillard, S. Giorgion and M. P. Pileni // *Adv. Mater.* **15** (2002) 1084.
[18] S. Chen and D. L. Carroll // *J. Phys. Chem. B* **108** (2004) 5500.
[19] Z. R. Tian, J. Liu, J. A. Voigt, H. Xu and M. J. Mcdermott // *Nano Lett.* **3** (2003) 89.
[20] M. C. Daniel and D. Astruc // *Chem. Rev.* **10** (2003) 1021.
[21] G. M. Whitesides, J. P. Mathias and C. T. Seto // *Science*, **254** (1991) 1312.
[22] Y. Sun, B. Mayers, T. Herricks and Y. Xia // *Nano Lett.* **3** (2003) 955.
[23] B. Yin, H. Ma, S. Wang and S. Chen // *J. Phys. Chem. B* **107** (2003) 8898.
[24] M. P. Pileni // *Nat.Mater.* **2** (2003) 145.
[25] Y. Y. Yu, S. S. Chang, C. L. Lee and C. R. C. Wang // *J. Phys. Chem. B* **101** (1997) 6661.
[26] S. Link, M. B. Mohamed and M. A. El-Sayed // *J. Phys. Chem. B* **103** (1999) 3073.
[27] N. R. Jana, L. Gearheart and C. J. Murphy // *J. Phys. Chem. B* **105** (2001) 4065.
[28] N. R. Jana, L. Gearheart and C. J. Murphy // *Chem. Commun.* **7** (2001) 617.
[29] F. Kim, J. Song and P. Yang // *J. Am. Chem. Soc.* **124** (2002) 14316.
[30] A. Kameo, A. Suzuki, K. Torigoe and K. Esumi // *J. Colloid Interf. Sci.* **241** (2001) 289.
[31] C. J. Johnson, E. Dujardin, S. A. Davis, C. J. Murphy and S. Mann // *J. Mater. Chem.* **12** (2002) 1765.
[32] P. L. Gai and M. A. Harmer // *Nano Lett.* **2** (2002) 771.
[33] R. Wang, J. Yang, Z. Zheng, M. D. Carducci, J. Jiao and S. Seraphin // *Angew. Chem. Int. Ed.* **40** (2001) 549.
[34] R. M. Crooks, M. Zhao and L. Sun // *Chem. Res.* **34** (2001) 181.
[35] M. Zhao, L. Sun and R. M. Crooks // *J. Am. Chem. Soc.* **120** (1998) 4877.
[36] L. Balogh and D. A. Tomalia // *J. Am. Chem. Soc.* **120** (1998) 7355.
[37] M. F. Ottaviani, F. Montalti, N. J. Turro and D. A. Tomalia // *J. Phys. Chem. B* **101** (1997) 158.
[38] T.S. Ahmadi, Z. L. Wang, T. C. Green, A. Henglein and M. A. El-Sayed // *Science* **272** (1996) 1924.
[39] M. Zhao and R. M. Crooks // *Adv. Mater.* **11** (1999) 217.
[40] J. Won, K.J. Ihn and Y. S. Kang // *Langmuir* **18** (2002) 8246.
[41] K. Esumi, R. Nakamura, A. Suzuki and K. Torigoe // *Langmuir* **16** (2000) 7824.
[42] Y. Sun and Xia // *Chem. Mater.* **14** (2002) 4736.
[43] L. D. Marks // *Rep. Prog. Phys.* **57** (1994) 603.
[44] Y. Gao, P. Jiang, D. F. Liu, H. J. Yuan, X. Q. Yan, Z. P. Zhou, J. X. Wang, L. Song, L. F. Liu, W.Y. Zhou, G. Wang, C. Y. Wang and S. S. Xie // *J. Phys. Chem. B* **108** (2004) 12877.
[45] Z. Zhang, B. Zhao and J. Hu // *Solid State Chem.* **121** (1996) 105.
[46] I. Pastoriza-Santos, L. M. Liz-Marzan // *Langmuir* **18** (2002) 2888.
[47] G. Carotenuto, G. P. Peper and L. Nicolais // *Eur. Phys. J. B* **16** (2000) 11.
[48] G. Wei, C. Nan, Y. Deng and Y. Lin // *Chem. Mater.* **15** (2003) 4436.
[49] D. Zhang, L. Qi, J. Yang, J. Ma, H. Cheng and L. Huang // *Chem. Mater.* **16** (2004) 872.
[50] Y. Sun and Y. Xia // *Science* **298** (2002) 2176.
[51] Y. Zhou, S. H. Yu, C. Y. Wang, X. G. Li, Y. R. Zhu and Z. Y. Chen // *Adv. Mater.* **11** (1999) 850.
[52] X. Wang and Y. Chujo // *Chem. Comm.* **12** (2002) 1300.
[53] X. Wang and Y. Chujo // *Langmuir* **19** (2003) 6242.

[54] F. Favier, H. Liu and R. M. Penner // *Adv. Mater.* **13** (2001) 1567.
[55] R. He and X. Qian // *J. Mater. Chem.* **12** (2002) 3783.
[56] I. Pastoriza-Santos and L. M. Liz-Marzan // *Langmuir* **15** (1999) 948.
[57] R. Jin, Y. Cao, C. A. Mirkin, K. L. Kelly, G. C. Schatz and J. G. Zheng // *Science* **294** (2001) 1901.
[58] P. V. Kamat, M. Flumiani and G. V. Hartland // *J. Phys.Chem. B* **102** (1998) 3123.
[59] R. Jin, Y. C. Cao, E. Hao, G. S. Me. Traux, G. C. Schatz and C. A. Mirkin // *Nature* **425** (2003) 487.
[60] K. K. Caswell and C. J. Murphy // *Nano Lett.* **3** (2003) 667.
[61] Q. F. Zhou and Z. Xu // *J. Mater. Chem.* **12** (2002) 384.
[62] S. L. Westcott, S. J. Oldenburg, T. R. Lee and N. J. Halas // *Chem. Phys. Lett.* ***300*** (1999) 651.
[63] S. W. Kim, M. Kim, W. Y. Lee and T. Hyeon // *J. Am. Chem. Soc.* **124** (2002) 7642.
[64] Y. Sun and Y. Xia // *Anal. Chem.* **74** (2002) 5297.
[65] M. Ohmori and E. Matijevic // *J. Coll. Interface Sci.* **150** (1992) 594.
[66] D. Sarkar and N. J. Halas // *Phys. Rev. E* **56** (1997) 1102.
[67] A. E. Neeves and M. H. Birnboim // *J. Opt. Soc. Am. B* **6** (1989) 787.
[68] R. D. Averitt, D. Sarkar and N. J. Halas // *Phys. Re*V*. Lett.* **78** (1997) 4217.
[69] S. J. Oldenburg, R. D. Averitt, S. L. Westcott and N. J. Halas // *Chem.Phys. Lett.* **288** (1998) 243.
[70] F. Caruso, M. Spasova, V. Salgueirin, O. Maceira and L. M. Liz-Marzan // *Adv. Mater.* **13** (2001) 1090.
[71] T. Ji, V. G. Lirtsman, Y. Avny and D. Davidov // *Adv. Mater.* **13** (2001) 1253.
[72] Y. Sun, B. T. Mayers and Y. Xia // *Nano Letters* **2** (2002) 481.
[73] Y. Sun and Y. Xia // *Nano Lett.* **3** (2003) 1569.
[74] N. R. Jana, L. Gearheart and C. J. Murphy // *J. Phys. Chem. B* **105** (2001) 4065.
[75] C. J. Murphy and N. R. Jana // *Adv. Mater*. **14** (2002) 80.
[76] M. Tornblom and U. Henriksson // *J. Phys. Chem. B* **101** (1997) 6028.
[77] S. O. Obare and C. J. Murphy // *Nano Lett.* **1** (2001) 601.
[78] B. D. Busbee, S. O. Obare and C. J. Murphy // *Adv. Mater.* **15** (2003) 414.
[79] T. Pal, S. De, N. R. Jana, N. Pradhan, R. Mandal, A. Pal, A. E. Beezer and J. C. Mitchell // *Langmuir* **14** (1998) 4724.
[80] T. K. Sau and C. J. Murphy // *Langmuir* **20** (2004) 6414.
[81] S. Chen, Z. L. Wang, J. Ballato, S. H. Foulger and D. L. Carroll // *J. Am. Chem. Soc.* **125** (2003) 16186.
[82] Z. Liu, Y. Yang, J. Liang, Z. Hu, S. Li, S. Peng and Y. Qian // *J. Phys. Chem. B* **107** (2003) 12658.
[83] X. Cao, F. Yu, L. Li, Z. Yao and Y. Xie // *J. Cryst. Growth* **254** (2003) 164.
[84] B. T. Mayers, K. Liu, D. Sunderland and Y. Xia // *Chem. Mater.* **15** (2003) 3852.
[85] B. Gates, Y. Yin and Y. Xia // *J. Am. Chem. Soc.* **122** (2000) 12582.
[86] B. Gates, B. Mayers, B. Cattle and Y. Xia // *Adv. Func. Mater.* **12** (2002) 219.
[87] B. Mayers, X. Jiang, D. Sunderland, B. Cattle and Y. Xia // *J. Am. Chem. Soc.* **125** (2003) 13364.
[88] Y. Wang, X. Jiang, T. Herricks and Y. Xia // *J. Phys. Chem. B* **108** (2004) 8631.
[89] S. Sun, C. B. Murray, D. Weller, L. Folks and A. Moser // *Science* **287** (2000) 1989.
[90] K. S. Suslick, M. Fang and T. Hyeon // *J. Am. Chem. Soc.***118** (1996) 11960.
[91] F. Dumestre, B. Chaudret, C. Amiens, P. Renaud and P. Fejes // *Science* **303** (2004) 821.
[92] K. Esumi, R. Isono and T. Yoshimura // *Langmuir* **20** (2004) 237.
[93] L. Yang, Y. Luo, X. Jia, Y. Ji, L. You and Q. Zhou // *J. Phys. Chem. B* **108** (2004) 1176.
[94] Y. Kim, S. Oh and R. M. Crooks // *Chem. Mater.* **16** (2004) 167.
[95] K. R. Gopidas, J. K. Whitesell and M. A. Fox // *J. Am. Chem. Soc.* **125** (2003) 14168.
[96] K. R. Gopidas, J. K. Whitesell and M. A. Fox // *Nano Lett.* **3** (2003) 1757.
[97] R. W. J. Scott, H. Ye, R. R. Henriquez and R. M. Crooks // *Chem. Mater.* **15** (2003) 3873.
[98] S. Oh, Y. Kim, H. Ye and R. M. Crooks // *Langmuir* **19** (2003) 10420.
[99] C. Z. Li, H. X. He, A. Bogozi, J. S. Bunch and N. J. Tao // *Appl. Phys. Lett.* **76** (2000) 1333.
[100] P. N. Bartlett and S. Guerin // *Anal. Chem.* **75** (2003) 126.